Biomaterials 33 (2012) 7834–7848

Contents lists available at SciVerse ScienceDirect

Biomaterials

journal homepage: www.elsevier.com/locate/biomaterials

Cellular uptake pathways of lipid-modified cationic polymers in gene delivery to primary cells

Charlie Y.M. Hsu [a], Hasan Uludağ [a,b,c,*]

[a] Department of Biomedical Engineering, Faculty of Medicine and Dentistry, University of Alberta, Edmonton, Alberta, Canada T6G 2V2
[b] Department of Chemical and Materials Engineering, Faculty of Engineering, University of Alberta, Edmonton, Alberta, Canada T6G 2G6
[c] Faculty of Pharmacy & Pharmaceutical Sciences, University of Alberta, Edmonton, Alberta, Canada T6G 2G6

ARTICLE INFO

Article history:
Received 16 May 2012
Accepted 29 June 2012
Available online 9 August 2012

Keywords:
Gene delivery
Uptake pathways
Endosome
Transfection
Nonviral vectors
Plasmid DNA

ABSTRACT

Hydrophobic modifications have emerged as a promising approach to improve the efficiency of non-viral gene delivery vectors (GDV). Functional GDVs from non-toxic polymers have been created with this approach but the mechanism(s) behind lipid-mediated enhancement in transfection remains to be clarified. Using a linoleic acid-substituted 2 kDa polyethylenimine (PEI2LA), we aimed to define the cellular uptake pathways and intracellular trafficking of plasmid DNA in normal human foreskin fibroblast cells. Several pharmacological compounds were applied to selectively inhibit uptake by clathrin-mediated endocytosis (CME), caveolin-mediated endocytosis (CvME) and macropinocytosis. We found that PEI2LA complexes were taken up predominantly through CME, and to a lesser extent by CvME. In contrast, its precursor molecule, PEI2 complexes was internalized primarily by CvME and macropinocytosis. The commonly used 25 kDa PEI 25 complexes utilized all endocytic pathways, suggesting its efficiency is derived from a different set of transfection pathways than PEI2LA. We further applied several endosome disruptive agents and found that hypertonic media enhanced the transfection of PEI2LA by 6.5-fold. We infer that lipid substitution changes the normal uptake pathways significantly and transfection with hydrophobically modified GDVs may be further enhanced by incorporating endosome disruptive elements into vector design.

1. Introduction

Cellular delivery of exogenous DNA molecules to manipulate physiological functions at the genetic level has been an indispensable tool in both molecular biology studies and biotechnology applications. Clinical translation of gene delivery as a form of molecular therapy has been slow to progress largely due to the absence of gene delivery vectors (GDVs) that can satisfy both efficiency and safety requirements. Dis-armed recombinant viral vectors remain as the most efficient method of gene delivery at present. However, the risk of immunogenicity, residual infectivity and insertional mutagenesis currently precludes their wide spread use [1]. Ongoing efforts into the development of non-viral GDVs have yielded a large library of biocompatible materials capable with sufficient DNA packaging and delivery ability in pre-clinical models, but they have yet to achieve the efficacy that viral vectors are able to incite. Strategies to improve the efficiency and biocompatibility of cationic reagents for gene delivery typically involve grafting functional ligands such as peptides, lipids, sugars, or a combination thereof, to improve stability, targeting, uptake and sub-cellular trafficking capabilities of the vectors [2]. In that regard, hydrophobic modification of cationic reagents with lipid moieties was shown to improve membrane binding and enhance gene delivery efficiency [3]. Our group has demonstrated the feasibility of this approach by grafting several endogenous lipids to the low molecular weight (2 kDa) polyethylenimine (PEI2). The most effective polymer, namely linoleic acid substituted PEI2 (PEI2LA), displayed markedly enhanced transfection efficiency over its relatively ineffective precursor molecule in both cultured cell lines and tissue-derived primary cells [4,5]. We previously showed that the enhanced efficiency of PEI2LA was partly due to stronger

* Corresponding author. Department of Chemical and Materials Engineering, Faculty of Engineering, University of Alberta, Edmonton, Alberta, Canada T6G 2G6. Tel.: +1 780 492 0988; fax: +1 780 492 2881.
E-mail address: hasan.uludag@ualberta.ca (H. Uludağ).

0142-9612/$ – see front matter © 2012 Elsevier Ltd. All rights reserved.
http://dx.doi.org/10.1016/j.biomaterials.2012.06.093

association with the nuclear membrane, which was correlated with better nuclear uptake and subsequent transgene expression [5]. However, the specific uptake pathway employed as well as the subsequent intracellular trafficking events mediated by the PEI2LA remain to be elucidated.

Lipid substitution is expected to enhance gene delivery by promoting stronger binding of the polymer/DNA complexes to hydrophobic domains of the plasma membrane to increase uptake. Hydrophobic modifications can also alter the physicochemical properties of the complexes, leading to a change in the uptake pathways. Uptake pathways are vitally important in determining the efficiency of GDVs as it relates to the intracellular processing, trafficking and recycling of the internalized complexes. Uptake of assembled complexes are widely regarded to proceed via endocytosis [6,7]. Endocytosis is broadly defined into two categories, pinocytosis and phagocytosis, the latter of which is restricted to specialized cell types such as lymphocytes and macrophages. Pinocytosis is further sub-divided into clathrin-dependent endocytosis (CME), caveolin-mediated endocytosis (CvME), macropinocytosis, and clathrin-/caveolin-independent pathway. CvME was thought to be the uptake pathway most conducive to transfection owing to its non-acidic, non-degradative environment, which maintained the intracellular integrity of the nucleic acid cargo. CvME was shown to be the endocytic pathway leading to efficient transgene expression in COS-7 and HeLa cells for PEI-mediated transfection [8–10]. However, others suggested the CME as the most efficient uptake pathway, as it not only provided an acidic environment for PEI complexes to facilitate endosome disruption via the proton-sponge effect, but also facilitated movement of the transgene cargo proximal to the perinuclear region, which subsequently increased the propensity for nuclear import [11]. Yet, recent studies have also suggested that uptake via macropinocytosis is the most efficient route of entry leading to transfection in PEI25 [12]. Regardless of which endocytic pathway is the most effective route for transfection, the notion that a single pathway can be optimal for all GDVs may not be realistic. Transfection pathways vary among different cell types [13,14] and are likely to depend on the biochemical nature of the GDVs and the physicochemical properties of resulting complexes [15]. In that regard, mechanistic studies and further design optimizations for non-viral GDVs should be ideally investigated in clinically relevant primary cell lines so that clinical translation to both *ex vivo* and *in vivo* delivery settings can be streamlined. That was not the case for previous studies exploring the role of endocytic pathways on the efficiency of non-viral GDVs, where transformed cell lines were routinely used [8,9,13,14,16–18].

In this study, we employed normal human foreskin fibroblast (NHFF) cells to elucidate the mechanism of cell entry and trafficking of polymeric GDVs. NHFF cell is a versatile platform in this regard since it has clinical relevance in both cell-based therapy for the induction of pluripotent cells and in cutaneous gene therapy for skin regeneration and wound repair [19–22]. We aimed to identify the predominant endocytic pathway involved in the uptake of PEI2LA complexes in NHFF cells as compared to native PEIs (PEI2 and PEI25). We applied a series of pharmacological inhibitors that selectively inhibited CME, CvME and macropinocytosis to determine the uptake pathway by reduction. The specific activities of the inhibitors were defined by titrating the concentrations of the drug against cell viability and transfection efficiency. We further examined the intracellular distribution of the complexes and the role of endosome release as a rate-limiting step in the overall transfection. Conclusions derived from this study would not only provide mechanistic insight into the impact of lipid-moieties in GDV trafficking but would also have direct implication on the future design of polymeric GDVs for therapeutic gene delivery to NHFF cells.

2. Materials and methods

2.1. Materials

The 2 kDa branched PEI (PEI2; $M_n = 1.8$ kDa, $M_w = 2.0$ kDa), 25 kDa branched PEI (PEI25; $M_n = 10$ kDa; $M_w = 25$ kDa), Hanks' Balanced Salt Solution (HBSS, with phenol red), (3-(4,5-dimethylthiazol-2-yl)-2,5-diphenyltetrazolium bromide (MTT), spectrophotometric-grade dimethylsulfoxide (DMSO), sucrose, chloroquine diphosphate salt, chlorpromazine hydrochloride, methyl-β-cyclodextrin (mβCD), genistein and trypsin/EDTA were obtained from SIGMA (St. Louis, MO). The PEI2LA was prepared according to the synthetic scheme outlined in [4], with LA:PEI2 feed ratio of 0.1, that gave a polymer with an average substitution of 1.2 linoleic acids per polymer. Opti-MEM® I Reduced Serum Media, Dulbecco's Modified Eagle Medium (DMEM; high and low glucose with L-glutamine), penicillin (10,000 U/ml), streptomycin (10 mg/ml) and non-essential amino acids (100×) were from Invitrogen (Grand Island, NY). Fetal bovine serum (FBS) was from PAA Laboratories (Etobicoke, Ontario). The blank plasmid gWIZ (i.e., no functional gene product) and gWIZ-GFP (i.e., Green Fluorescent Protein mammalian expression plasmid) were purchased from Aldevron (Fargo, ND). The photosensitizer aluminium phthalocyanine disulfonate (AlPcS2a) was purchased from Frontier Scientific (Logan, UT, USA). Wortmannin and amiloride hydrochloride were obtained from Santa Cruz Biotechnology (Santa Cruz, CA). Hoechst 33258, Pentahydrate (bis-Benzimide) and Alexa Fluor® 488 labeled Dextran (10 kDa) were from Life Technologies (Burlington, ON).

2.2. Cell culture

NHFF cells were isolated from patients as described previously [23] and cultured in a basic growth medium comprised of DMEM containing 4.5 g/ml D-glucose, supplemented with 10% heat inactivated fetal bovine serum (FBS), 2 mM l-glutamine, 0.1 mM MEM non-essential amino acids, 100 U/ml penicillin, and 100 μg/L of streptomycin. Cells were maintained in a humidified 37 °C incubator with 5% CO_2. NHFF cells passaged between 14 and 24 generations were used in this study, and were grown in multiwell plates for transfection studies. For both uptake and transfection studies, cells were seeded in 24-well plates at an initial seeding density of 3×10^5 cells/well.

2.3. Plasmid DNA (pDNA) labeling

The gWIZ-GFP plasmid is a 5757 bp mammalian expression plasmid, which contains a modified promoter from the human cytomegalovirus (CMV) immediate early (IE) genes. gWIZ-GFP was labeled with the fluorophore Cy3 using the Label IT® Tracker™ Intracellular Nucleic Acid Localization Kit (Mirus Bio, WI) as per manufacturer's instructions. Briefly, a 0.2 (v/w) ratio of dye to nucleic acid reaction mix was prepared and incubated at 37 °C for 90 min. Unbound free Cy3 molecules were removed by ethanol precipitation according to manufacture suggested protocol. Purified labeled pDNA was then suspended in ddH_2O. Labeling efficiency was determined by calculating the ratio of base to dye using the equation $(A_{base} * \varepsilon_{dye})/(A_{dye} * \varepsilon_{base})$ by measuring absorbance at 260 nm (base) and 550 nm (dye) using the values $\varepsilon_{Cy3} = 250{,}000$; $\varepsilon_{base} = 6600$ and $CF_{260} = 0.05$. The contribution of dye to the A_{260} reading was corrected by using the equation $A_{base} = A_{260} - (A_{dye} * CF_{260})$. Plasmid DNA labeled using the concentration outlined yielded approximately 300 Cy3 labels per pDNA.

2.4. Cytotoxicity assessment of endocytosis inhibitors by MTT assay

The cytotoxic effects of the uptake inhibitors were assessed using the MTT cell viability assay, in which the yellow tetrazolium salt (MTT) is reduced in metabolically active cells to form insoluble purple formazan crystals, which are solubilized by the addition of DMSO. Briefly, NHFF cells were seeded in 48-well plates at a concentration of 1×10^5 cells/well. Once the cells reached a density of 50–60% or after 1–2 days, inhibitors were added and incubated in OPTI-MEM. After 4 h incubation, inhibitors were removed and cells were further incubated for an additional 20 h in fresh growth medium. To process cells for assay, MTT was added directly to the medium to a final concentration of 1 mg/ml, and incubated at 37 °C for 2 h; the supernatant was removed by inverting the plates to decant the liquid; crystals remaining at the bottom of the plate were dissolved in DMSO at 200 μl/well. The absorbance was measured at 570 nm using an ELx800 absorbance microplate reader (Bio-Tek, Winooski, VT). Cell viability was expressed as a percentage relative to untreated cells, which served as the control.

2.5. Preparation of complexes for transfection

Self-assembled polymer/pDNA complexes were formed by diluting pDNA and polymer solutions separately in equal volumes of salt-free buffer (20 mM HEPES, pH 7.4) for PEI25 and PEI2 or OPTI-MEM for PEI2LA. After 5 min of equilibration, the pDNA and polymer solutions were mixed together, vortexed for 5 s, and incubated at room temperature for 25 min. The volume of the complexes at this stage was 1/5 of the final transfection media volume (i.e., 100 μl complex volume in a total of 500 μl

tissue culture medium per 24-well). The polyplex solutions were then diluted 1:5 in OPTI-MEM to bring the final pDNA concentration to 2 μg/ml per well and added directly to each well; plates were then centrifuged at 210 × g for 5 min (acceleration and deceleration set to lowest setting) to force the complexes onto the cell surface. All transfection and uptake studies included this centrifugation step following the addition of complexes.

2.6. Transfection efficiency and gene expression kinetics

For gene expression kinetics, complexes were prepared for transfection was as described above. After 4 h incubation, complexes were removed and replaced with growth medium. At the designated time point, cells were processed for flow cytometry by first washing with Ca^{2+}/Mg^{2+} free HBSS (without phenol red; CMF-HBSS) for ~5 min to remove residual divalent cations then detached by enzymatic treatment by incubating with clear 0.01% Trypsin/EDTA for 1–2 min. After gentle tapping and shaking, detached cells were fixed in 3.7% formalin in HBSS.

For transfection studies involving the inhibitors, cells were pre-treated with the inhibitors diluted in OPTI-MEM to the concentrations outlined in the figures (400 μl were dispensed into each well in a 24-well plate). After 2 h incubation, 100 μl of complexes were added directly to each well (final DNA concentration at 2 μg/ml), then centrifuged as described above and incubated in the presence of the inhibitors for an additional 4 h; transfection complexes were subsequently removed and replaced with growth media. GFP expression was assayed 20 h later by processing cells for flow cytometry analysis on a Beckman Coulter Cell Lab Quanta with MPL Option (Missisauga, ON) equipped with a 488 nm laser diode and standard filter (460 BP, 525 BP, 575 BP and 670 LP).

To investigate the effect of chloroquine on transfection, cells were pre-treated with 40 μM chloroquine for 2 h prior to transfection. This concentration was empirically determined to give the overall highest increase in mean fluorescence without significant reduction in cell viability (data not shown). For light-induced endosome disruption, cells were pre-loaded with the photosensitizer (PS) by incubating cells with 5 μg/ml of AlPcS2a in growth media for 16 h. Then cells were washed (×3) with growth media and chased for 2 h in PS-free media to remove surface-bound PS before transfection. After incubation with transfection complexes for 3 h, cells were exposed to light emitted by a bank of six T5 wide-spectrum high output fluorescent lamps (F54T5/841) placed at 30 cm directly above the plate for 45 s, then placed back in the incubator for an additional 3 h before complexes were removed and replaced with growth media. The utilized concentration of AlPcS2a and light dose were empirically determined by titrating a range of concentrations (1, 2, 5, and 10 μg/ml) and exposure time (30, 45, 60, 90 and 120 s) against transfection efficiencies (data not shown). To investigate the effect of hypertonic media on transfection, cells were incubated in 0.45 M sucrose dissolved in serum-free OPTI-MEM for 2 h prior to transfection. In all cases, expression of GFP was assayed 24 h later by flow cytometry.

Analysis for transfection efficiency was performed by calibrating the gated regions such that the negative control (i.e., polymer complexes prepared with gWIZ) had 1% auto-fluorescent cells. Transfection efficiency was expressed in terms of the mean fluorescent intensity value captured in the FL1 channel. The relative transfection efficiency was expressed as a percentage of untreated cells.

2.7. Uptake kinetics and inhibition of endocytosis

For measurement of uptake kinetics, Cy3-labeled pDNA (Cy3-pDNA) was used to quantitate the amount of intracellular pDNA. Cells were seeded in 24-well plates and transfected as above; Cy3-pDNA were mixed with unlabeled pDNA at a 1:1 ratio (transfection efficiency of the mixture in 293T cells was ~90% based on GFP-positive cells, or ~70% based on mean GFP expression relative to unlabeled plasmid; unpublished). Prior to the prescribed time point for analysis, complexes were removed, and cells were washed twice with growth media, then chased for 30 min in label-free media to allow residual complexes to be internalized. Cells were then detached by trypsin and suspended in 3.7% formalin for flow cytometry. Quantification of Cy3-pDNA uptake was performed by taking the mean fluorescent values from the FL2 channel, calibrated to 1% auto-fluorescence in cells transfected with unlabeled gWIZ complexes.

For uptake studies in the presence of endocytosis inhibitors, cells were pre-treated for 2 h with the inhibitors diluted in OPTI-MEM to the concentrations outlined in the results section (400 μl were dispensed into each well in a 24-well plate). Then, complexes were prepared as described above (in 100 μl) and added directly to each well (final concentration of pDNA was 2 μg/ml), then centrifuged as described above and incubated in the presence of the inhibitors for an additional 4 h. Afterward, complexes were removed, cells were washed with growth media (×2) and further chased in dye-free growth media for an additional 2 h to allow residual complexes to be detached or internalized. Removal of surface-bound complexes was verified by microscopy (data not shown). Relative percentage of uptake was expressed in terms of transfected cells that were not exposed to the inhibitors (buffers only).

2.8. Laser scanning confocal fluorescent microscopy

NHFF cells were seeded onto a 12-well tissue culture plates at 3×10^6 cells/well. Once attached and cell density has reached ~60–70%, endosomes were labeled by incubating the cells for 16 h in the presence of 500 μg/ml of Dextran-Alexa Fluor® 488, diluted in cell media. Cells were then washed twice in dye-free media then transfected as described above. After 4 h incubation, complexes were removed, washed twice with basic medium and chased in dye-free medium for 30 min. Cells were then washed with CMF-HBSS (×2) and fixed in 3.7% formalin for 15 min. Nuclei were stained with Hoechst 33258 (300 nm/ml in HBSS). Prior to imaging, CMF-HBSS was replaced with a glycerol mixture containing 9:1 glycerol-to-HBSS (v/v). 16-bit images were acquired using an inverted Zeiss LSM 710 Laser Scanning Confocal Microscope (Carl Zeiss, Oberkochen, Germany) through a 10 × 0.45NA EC Plan-Neofluar objective lens with a field view of 125.03 μm × 125.03 μm at 0.08 μm/pixel. Nuclei stained with Hoechst were visualized by excitation at 405 nm, while Dextran-Alexa Fluor® 488 and Cy3-pDNA were excited at 488 nm and at 561 nm, respectively.

For live-cell imaging, cells were seeded onto a glass bottom dish with a No. 1.5 coverglass (0.16–0.19 mm; MatTek Corporation, Ashland, MA). Cells were incubated with AlPcS2a (5 μg/ml) diluted in growth media for 16 h, then washed twice with growth media and transfected with Cy3-pDNA complexes as before. After 4 h incubation, transfection complexes were replaced with cell media, and the cells directly imaged on a Quorum WaveFX-X1 Spinning Disc Confocal System (Quorum Technologies Inc., Guelph, ON). Cells were staged in an environmentally controlled Chamlide TC-A Live Cell Chamber (37 °C incubator + 5% CO_2 atmosphere) fitted with a 35 mm micro-dish adaptor. Images were acquired through a 20X/0.75 dry lens and detected on a Hamamatsu EMCCD (C9100-13) with a voxel size of 0.499 μm/pixel (x, y). AlPcS2a was excited by a 45 mW 642 nm pumped diode laser while Cy3-DNA were visualized with 50 mW 561 nm pumped diode laser.

Wide-field fluorescent microscopy was performed on an Olympus FSX100 equipped with a metal halide lamp. Live-cell imaging of cells seeded in plastic tissue culture plates were acquired through the LCACHN40×PHP lens (NA0.55) at 20× magnification. Cy3-pDNA was visualized in the TRITC channel (BP530-550, BA575IF, DM570).

2.9. Particle size measurements

The hydrodynamic size range of the polymer/pDNA complexes was measured by photon correlation spectroscopy (Zetasizer Nano, Malvern Instruments Ltd, Worcestershire, UK). Polyplexes were prepared as above, at polymer-to-DNA weight ratios of 2.5 for PEI25, 10 for PEI2 and PEI2LA, then diluted to 1 ml in OPTI-MEM at a final DNA concentration of 2 μg/ml prior to measurement. Measurements were taken in a heated chamber at 37 °C and 660 nm wavelength, and particle sizes were calculated by using a medium viscosity of 1.140 cP and a refractive index of 1.333 (at 37 °C). Values reported were from an average of 12 measurements with 10 s interval between each measurement.

2.10. Statistical analysis

Where indicated, the data is summarized as the mean ± standard deviation of triplicate measurements. Unpaired Student's t-test was used to assess statistical differences ($p < 0.05$) between the group means. All experiments were done in triplicate with a minimum of three independent experiments.

3. Results

3.1. Particle sizes and transfection efficiencies in NHFF cells

We initially sought out to optimize the complexation conditions for each GDV so that subsequent uptake and trafficking studies are investigated under optimal conditions that accurately reflect the transfection capability of each GDV. Based on an optimization procedure outlined [24], we found that PEI2LA complexes prepared in OPTI-MEM transfected more efficiently than those prepared in salt-free buffers (Supplement Fig. 1). The opposite trend was observed for PEI25 and PEI2 complexes, in which salt-free buffers favored formation of more effective complexes. Using the optimized conditions, transfection efficiencies in NHFF at various polymer-to-DNA weight ratios (w/w) are summarized in Fig. 1. At a weight ratio of 10, the mean GFP fluorescence of PEI2LA transfected cells was 5-fold higher than those transfected by PEI2. PEI25 was the most effective GDV yielding 1.4-fold and 7-fold higher reporter gene expression than PEI2LA and PEI2, respectively. Transfection efficiencies were dependent on the weight ratio; 2.5 was most effective for PEI25, which is equivalent to a nitrogen-to-

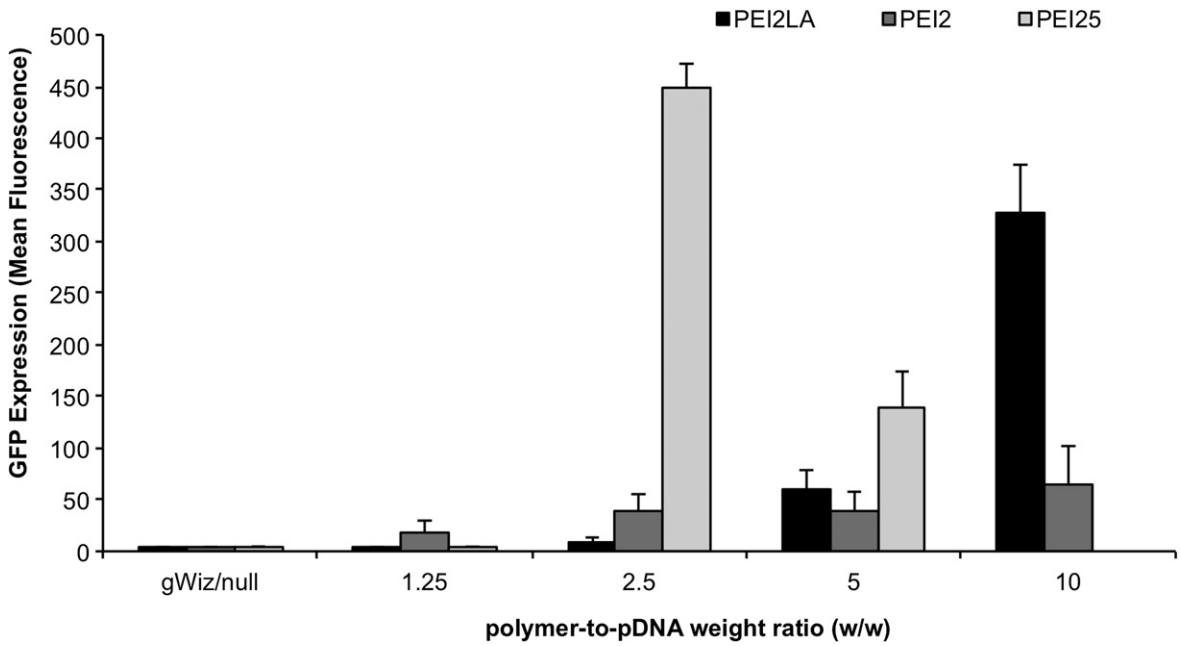

Fig. 1. Transfection efficiency of PEI2LA, PEI25 and PEI2 in NHFF cells at various polymer-to-pDNA weight ratios. Bar height depicts the mean cellular fluorescence in the FL1 channel. The efficiency of PEI25 was optimal at a weight ratio of 2.5 while the efficiency of PEI2 and PEI2LA was optimal at a weight ratio of 10. GFP expression in PEI2LA-transfected cells was 5-fold higher than those transfected by PEI2. PEI25 at a ratio of 10 was toxic and no data could be collected.

phosphate (NP) ratio of 19.35, while a ratio of 10 (NP = ~75.5, assuming a similar MW for these two polymers) was optimal for both PEI2 and PEI2LA. These weight ratios were employed for the subsequent studies.

We further measured the mean hydrodynamic sizes of the complexes at the weight ratios optimal for transfection. PEI2LA complexes prepared at a weight ratio of 10 averaged around 570 nm with >75% in the 530–615 nm range (Fig. 2); PEI2 complexes were smaller and exhibited a broader size distribution compared to PEI2LA, where most complexes were in the 295–531 nm range. PEI25 complexes were the smallest, with ~80% falling within the 164–255 nm range.

3.2. Uptake kinetics of pDNA

The pDNA uptake studies were conducted by using Cy3 as the fluorophore for pDNA labeling since its fluorescence is relatively insensitive to pH changes that occur in the endosomes. Visual assessment of cellular uptake under wide-field fluorescent microscope showed differences in fluorescent intensities among the three complexes (Fig. 3a), where PEI2LA complexes were 27 much brighter than PEI2 and PEI25 complexes. Quantification of fluorescence of the complexes showed that PEI25 complexes had intensity similar to free pDNA whereas PEI2 and PEI2LA complexes were 2 and 2.5 times brighter (Fig. 3b). Accordingly, we did not use fluorescence intensity as a measure of relative uptake efficiency. The relative sizes of the complexes as seen under microscopy (Fig. 3a) were also consistent with sizes measured by DLS, in which PEI2LA complexes were noticeably larger than the complexes seen in PEI25.

The kinetics of complex uptake was determined to provide insights into the uptake pathways, since the rate of internalization is pathway dependent. CME is considered to be a rapid process (<10 min), whereas uptake via CvME or macropinocytosis tend to

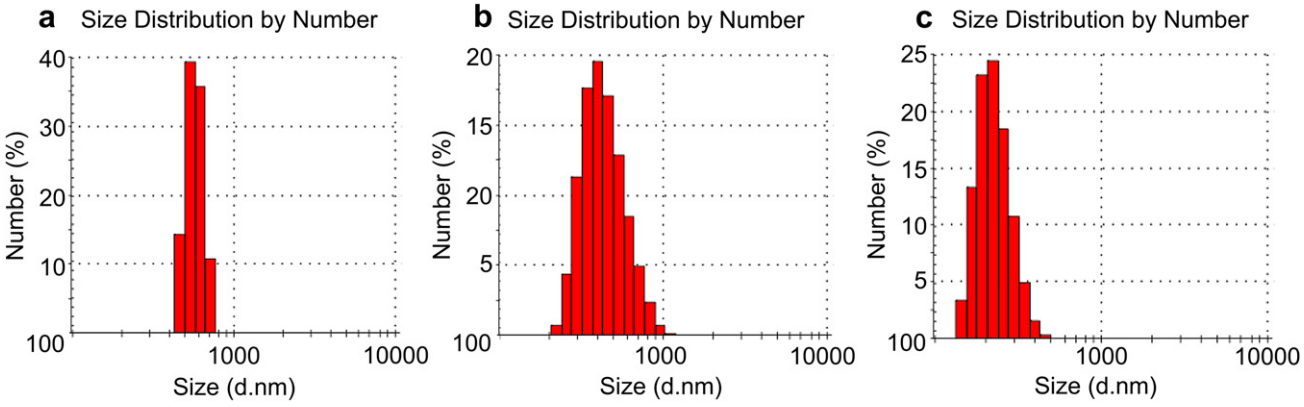

Fig. 2. a) Hydrodynamic size ranges of complexes formulated with PEI2LA in OPTI-MEM. The sizes of the particles in terms of proportional make up is as follows (in nm): 458.7, 14.3%; 531.2, 39.3%; 615.1, 35.7%; 712.4, 10.7%). b) Hydrodynamic size ranges of complexes formulated with PEI2 in salt-free buffer. Size distribution (nm): 220.2, 0.7%; 255, 4.3%; 295.3, 11.3%; 342, 17.6%; 396.1, 19.5%; 458.7, 17.1%; 531.2, 12.8%; 615.1, 8.5%; 712.4, 5.0%; 825.0, 2.3%; 955.4, 0.7%; 1106, 0.1%). c) Hydrodynamic size ranges of complexes formulated with PEI25 in salt-free buffer. Size distribution (nm): 141.8, 3.3%; 164.2, 13.3%; 190.1, 23.2%; 220.2, 24.5%; 255, 18.4%; 295.3, 10.7%; 342, 4.8%; 396.1, 1.5%; 458.7, 0.2%.

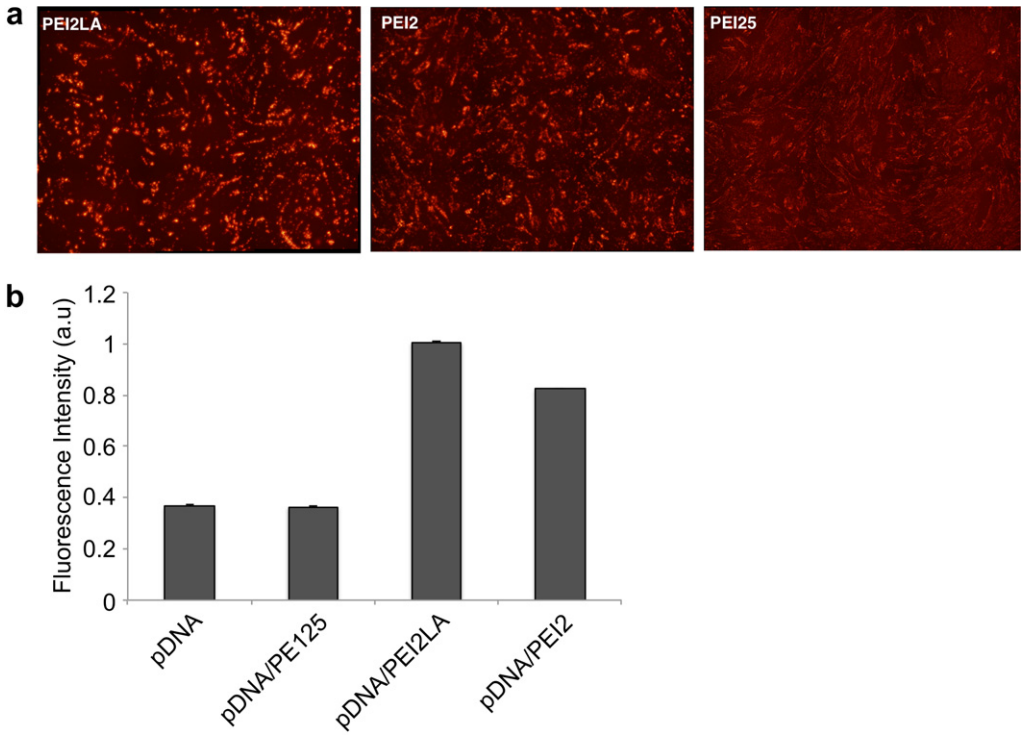

Fig. 3. Fluorescent intensity of PEI2LA, PEI2 and PEI25 complexes. a) PEI2LA complexes (left pane) were brighter under fluorescent microscope as judged by the difference between the signal and background. The fluorescent intensity of PEI2 complexes (middle pane) and PEI25 (right pane) was noticeably dimmer than PEI2LA. b) Quantitative measurement of the fluorescence of pDNA/polymer particles by a plate reader using the 544/590 nm filter pair.

exhibit slower kinetics (>20 min [25]). Fig. 4 shows the uptake of the Cy3-pDNA/complexes over time, expressed as a percentage of the highest uptake, which was reached at different time points for each of the GDV. Uptake of PEI2LA complexes reached a saturation maximum at 2 h, followed by PEI25 and PEI2 complexes at 3 and 4 h, respectively. Furthermore, within 15 min of incubation, uptake of PEI2LA complexes was already at 70% of maximum, compared to 37% and 40% for PEI25 and PEI2 complexes. Therefore, we infer that

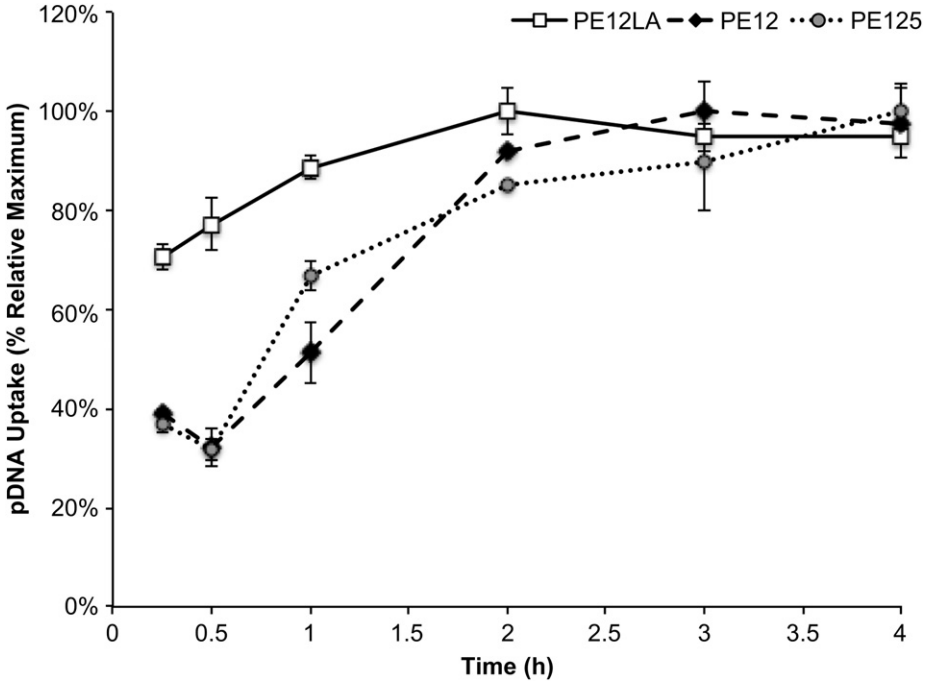

Fig. 4. Uptake kinetics of PEI2LA, PEI25 and PEI2 complexes in NHFF cells. Prior to the designated time point, transfection complexes were removed and cells were chased in dye-free for 30 min before processing for flow cytometry. Values are represented as a percent of maximum, which took place at 2, 3, and 4 h for PEI2LA, PEI25 and PEI2 complexes, respectively. The level of uptake for PEI2LA reached 70% of maximum at 0.25 h, while PEI25 and PEI2 exhibited slower uptake kinetics, starting at 37% and 40%, respectively.

PEI2LA exhibited a faster rate of internalization than PEI2 and PEI25, which may suggest a greater involvement of CME during the uptake.

3.3. Transgene expression kinetics

The kinetics of transgene expression was determined to establish a time frame for intracellular trafficking events leading to gene expression. Fig. 5 shows the relative GFP expression over a 72 h period in which transgene expression was expressed as a percentage of the highest mean fluorescence for each GDV. Highest transgene expression for PEI2LA and PEI25 were observed at 16 h while PEI2 had maximal expression at 24 h. By 48 h, transgene expression dropped to 66%, 54% and 40% for PEI25, PEI2 and PE2LA, respectively. Hence, the majority of intracellular processes leading to transgene expression took place within the first 16–24 h. The gradual decline in GFP fluorescence suggested there was no additional transgene expression beyond the first 24 h, indicating a coupling between the transfection and uptake processes.

3.4. Effect of endocytosis inhibitors on transfection efficiency

To elucidate the endocytic pathways involved in the uptake of complexes, we employed a number of inhibitors that are specific to CME, CvM, and macropinocytosis (Table 1). Since the activity of the inhibitor is highly dependent on the cell type and the administered concentration [26], the effects of inhibitor were investigated over a practical range of concentrations to draw our conclusions. Fig. 6a and b show the effect of CvME inhibitors genistein and mβCD on transfection efficiency. Transfections by all three GDVs were strongly inhibited by genistein, with 50% reduction at 20 μM, reaching complete inhibition at 75 μM (Fig. 6a). A dose-dependent effect on transfection was evident for genistein, where increasing concentrations resulted in corresponding reductions in transgene expression. The effect of genistein did not appear to differ significantly among the GDVs and suggested an equal dependence on tyrosine phosphorylation for transfection. mβCD also had a dose-dependent effect on transfection (Fig. 6b), in which transfections were reduced by 50% above 4 μM. The effect of mβCD was heterogeneous on the cell population; even with >90% reduction in the number of transfected cells, there remained a few GFP-positive cells that displayed high fluorescence (data not shown). This accounts for the relatively large error bars in the figures, in which the overall fluorescence is represented by a few highly GFP-expressing cells. mβCD inhibited transfection by PEI2 (5% of control) to a greater extent than transfections by PEI2LA and PEI25 (34% and 23% of control, respectively), suggesting PEI2 complexes have higher dependence on lipid-raft mediated endocytosis for transfection. However, we noted that transfection efficiency of PEI2 was low to begin with, which may not provide the same quantitative resolution as PEI2LA and PEI25 when calculating relative transfection efficiency.

Fig. 6c shows the effect of CPZ on transfection efficiency. The inhibitory effect of CPZ on transfection started at 5 μg/ml; 7.5 μg/ml was the highest concentration that can be administered without causing significant toxicity (80% viability). CPZ reduced transfection by PEI2LA significantly more than PEI2 and PEI25 (86% vs. 50% and 70%, respectively), suggesting a proportionally greater involvement of CME in the uptake of PEI2LA complexes.

The effects of the macropinocytosis inhibitors amiloride and wortmannin on transfection efficiency are shown in Fig. 6d and e. The inhibitory effect of amiloride was greatest on PEI2-mediated transfection, which completely abolished transgene expression at 30 μM. In contrast, PEI2LA was least affected, with 42% reduction in GFP fluorescence. Similarly, wortmannin strongly reduced transfection by PEI2 and PEI25 to 20% and 8% of the control groups at 75 nM, respectively (Fig. 6e). PEI2LA again were least affected by the macropinocytic inhibitor wortmannin (50% reduction).

3.5. Effect of endocytosis inhibitors on pDNA uptake

Since the effect of the endocytosis inhibitors is dose-dependent, vital cellular processes may be compromised at high concentrations, leading to reduced cell viability and changes in uptake pathways in a non-specific manner. We assessed the cytotoxic effect of the inhibitors over a concentration range. The line graph overlay in Fig. 6

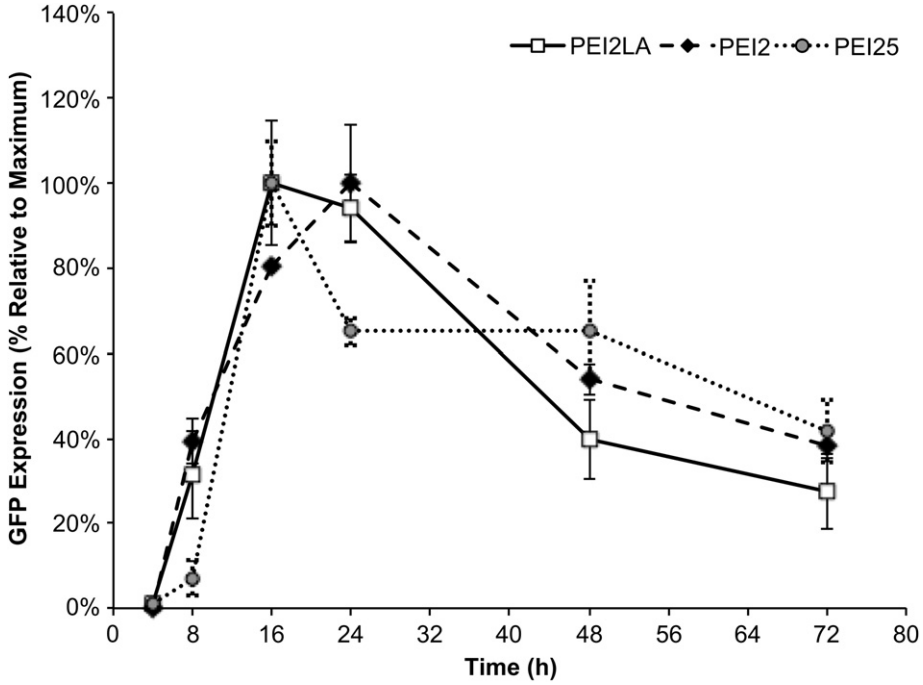

Fig. 5. Kinetics of GFP expression during the first 72 h following the transfection with complexes. Values are expressed as a percentage of the maximum, which was achieved at 16 h for PEI2LA and PEI2, and at 24 h for PEI25. GFP expression in transfected cells for the three GDVs gradually diminished after 24 h.

Table 1
List of inhibitors and endosome disruptors used in this study.

Drug	Mechanism of activity	Pathway	Concentration	Reference
Methyl-b-cyclodextrin (mβCD)	A cyclic oligomer of glucopyranoside, extracts cholesterol from the plasma membrane	CvME	8 μM	[58]
Genistein	Tyosine kinase inhibitor, blocks the phosphorylation of caveolin-1	CvME	75 nM	[59]
Chlorpromazine (CPZ)	A cationic amphiphilic drug, inhibits clathrin-coated pit formation by relocating clathrin and its adapter proteins from the plasma membrane to the endosomes	CME	7.5 μg/ml	[60]
Amiloride	Interferes with membrane Na+/H+-ATPase required for ruffling	Macro-pinocytosis	30 μM	[61]
Wortmannin	Inhibitor of phosphatidyl inositol-3-phosphate (PI3K)	Macro-pinocytosis	75 nM	[62]
AlPcS2a	Taken up via endocytosis and localized in endosome. Light irradiation induced oxidative damage to rupture endosomes	Endosome release	5 μg/ml; 45 s of light exposure	[27,63]
Chloroquine	Weak hydrophobic base, buffers acidification in early endosomes to prevent DNA degradation and promoting endosomal release of the cargo	Endosome release	40 uM	[7]
Sucrose	Hypertonic media, induces lysosomal swelling by increasing osmotic pressure within endosomes	Lysosome	0.45 M	[28,64]

depicts the percentage of viable cells at the same concentrations as those administered in the transfection studies. There was no significant toxicity from genistein or mβCD on NHFF cells for all concentrations tested. CPZ and amiloride had a dose-dependent effect on cell viability; 7.5 μg/ml and 30 μM of the drugs resulted in >50% reduction in cell number, respectively. Wortmannin also reduced cell number by 40% without a dose dependence. In addition to a decrease in viability, toxicity can be seen in the form of altered and irregular cell morphology for cells treated with amiloride and CPZ (not shown). Rather than the elongated shape typical of fibroblasts, treatment with these drugs resulted in shriveling and detachment from the surface, suggestive of necrosis. In light of recent work by Vercauteran et al. on the proper use of inhibitors to study endocytic pathways [26], concentrations for specific inhibitor were chosen based on securing a significant effect on transfection without an equivalent effect on cell viability. The chosen concentrations for subsequent uptake studies were 75 μM for genistein, 10 μM for mβCD, 7.5 μg/ml for CPZ, 30 μM for amiloride, and 75 nM for wortmannin.

The effect of inhibitors on pDNA uptake was measured 6 h after transfection and expressed as a percentage of untreated cells (Fig. 7). Treatment with mβCD significantly inhibited the uptake of all three complexes ($p < 0.05$); the extent of inhibition was greatest in PEI2 (45% vs. 26% and 24% for PEI2, PEI2LA and PEI25, respectively). Genistein interfered with the uptake of all three complexes as well, but the differences in uptake among the three GDVs were negligible. Wortmannin reduced the uptake of PEI2 and PEI25 complexes by 27% and 20%, respectively, but otherwise had no effect on PEI2LA complexes. Similarly, amiloride partially blocked the uptake of PEI2 and PEI25 by 35–40%, but had minimal effect on PEI2LA uptake. The CME-inhibitor CPZ significantly reduced the uptake of PEI2LA (38%) and PEI25 (31%) complexes, but not those of the PEI2 complexes (7%). Taken together, we infer that PEI25 complexes utilized a wide range of uptake pathways involving macropinocytosis, CME, and CvME. In contrast, PEI2 was taken up predominantly through macropinocytosis and CvME-mediated endocytosis. Linoleic acid substitution on PEI2 re-routed the entry pathways to predominantly CME, while engaging the CvME to some extent.

3.6. Effect of endosome disruption on transfection

We investigated the role of endosome entrapment on transfection efficiency using a number of complementary endosome disruptive methods. Chloroquine is a weak hydrophobic base that buffers acidification in endolysosomal compartments to promote endosomal release of pDNA [7]. Following 2 h pre-treatment with chloroquine, transfection by PEI2LA was increased by 50% (based on mean GFP fluorescence), but transfection of PEI2 and PEI25 complexes was reduced by 36% and 31%, respectively (Fig. 8).

We then employed the photosensitizer (PS), AlPcS2a to facilitate light-induced endosome disruption [27]. Endosomes were loaded with the PS by incubating cells with 5 μg/ml of AlPcS2a for 16 h prior to transfection. Transfected cells were then irradiated with a wide-spectrum light at 3 h after the addition of complexes; this time frame was empirically determined to give the most significant changes in transgene expression (data not shown). AlPcS2a-induced endosome release had a positive effect on transfection by PEI2LA and PEI2 complexes, increasing transgene expression by 60% and 49%, respectively (Fig. 8), but reduced the efficiency of PEI25 by 27%.

We further transfected the cells in 0.45 M sucrose, which is a hypertonic media that can cause intracellular cytoplasmic swelling within endosomes [28] to promote cytosolic release of endocytosed materials. The hypertonic media enhanced the transfection of PEI2LA complexes by 655% (based on mean GFP fluorescence), while PEI25 complexes displayed 60% increase and PEI2 complexes displayed 85% decrease.

Since endosomal transport is most commonly associated with CME, the effects of these endosome disruptive methods on the transfection efficiency of PEI2LA further suggest that uptake of PEI2LA proceeds predominantly through CME, and that endosome escape is a rate-limiting step in the transfection pathway of PEI2LA.

3.7. Intracellular distribution of complexes

To complement the quantitative results from flow cytometry, qualitative information on the intracellular distribution of complexes was generated using fluorescent microscopy. Fig. 9 shows CLSM images of cells transfected with Cy3-pDNA (red) complexes, with the nuclei and late endosomes/lysosomes stained with Hoechst 33528 (blue) and AF488-Dextran (green), respectively. The patterns of distribution in PEI2 resemble that of dextran-labeled endosomes, which coalesced into regions surrounding the nuclei (Fig. 9a). The shared patterns between AF488-Dextran and PEI2 complexes, however, did not appear to indicate co-localization, as the red and green punctates were distinctly separated. The distribution pattern of PEI2LA noticeably differed from

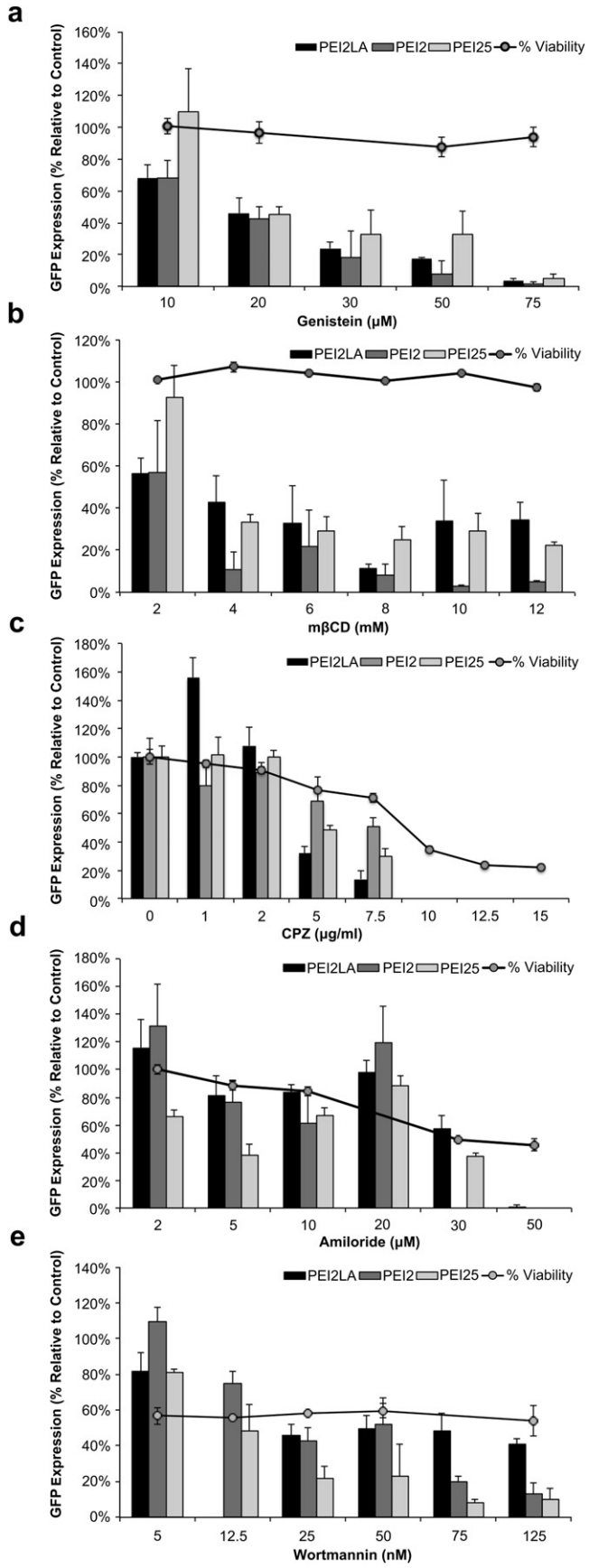

Fig. 6. The effect of the endocytic inhibitors genistein (a), mβCD (b), CPZ (c), amiloride (d), and wortmannin (e) on transfection efficiency. Bar graph denotes the relative mean fluorescent (FL1) of transfected cells treated with the indicated inhibitor as a percentage of control cells (without treatment with inhibitors). Line graphs denote the cell viability with inhibitor treatment at indicated concentrations as a percentage of untreated cells (no inhibitors).

PEI2 and appeared throughout the cell as large string-like aggregates (Fig. 9b). PEI25 complexes were much smaller, uniform in size and morphology, and were generally distributed randomly throughout the cell (Fig. 9c). Neither PEI2LA nor PEI25 appeared to be co-localized with AF488-Dextran. We also noted that the DNA-intercalating Hoechst dye bound to PEI2LA complexes more than PEI2 complexes (some binding) or PEI25 complexes (no binding), as evident by the purple colors in the composite image. This may suggest that DNA complexed with PEI2LA were more accessible to tertiary binding – a feature that may be beneficial for transgene expression, which require binding by transcription factors.

We further carried out confocal microscopy on transfected cells loaded with the photosensitizer AlPcS2a to gain insights into the observed transfection effects. Because AlPcS2a is extremely sensitive to light and is non-fixable, we employed spinning disk confocal microscopy to carry out live-cell imaging. Fig. 10 shows confocal images of transfected cells with AlPcS2a (cyan) and Cy3-pDNA (orange). Consistent with the fixed cell images acquired with CLSM above, PEI2 complexes tended to concentrate into defined regions, whereas PEI2LA and PEI25 complexes appeared more randomly distributed. AlPcS2a displayed a defined distribution pattern in which a hollow circular region can be negatively traced out by the exclusion of AlPcS2a from the area, suggestive of a perinuclear localization. The superimposed images indicated a low degree of co-localization between AlPcS2a and PEI2LA or PEI25 complexes, as evident by the exclusivity between the two colors. PEI2, appeared to share similar distribution pattern as AlPcS2a, but we were not able to collect z-stacks required for quantitative co-localization analysis, since AlPcS2a destabilized after just 20 s of laser exposure. Regardless, we can conclude by qualitative visual assessment that AlPcS2a had low degree of co-localization with the complexes, suggestive of distinct sets of uptake pathways for the molecules.

Given the significant increase in the transfection of PEI2LA under hypertonic conditions, we next examined the intracellular distribution of Cy3-pDNA in transfected cells treated with 0.45 M sucrose (Fig. 11). Untreated cells showed complexes in discrete regions of bright punctates and appeared more concentrated around the perinuclear region where a negative outline of the nucleus can be seen. In contrast, under hypertonic media, both PEI2 and PEI25 complexes appeared diffused, with lower signal-to-background ratio, which may be indicative of partially decondensed or dissociated complexes since free DNA showed lower fluorescence than complexes, as Fig. 3b indicated. Further, PEI2 and PEI25 complexes were more evenly distributed in sucrose treated cells, hinting a disruption to the endolysosomal trafficking, whereby released complexes were free to move within the cytoplasmic space. Despite the contrasting patterns noted in PEI2 and PEI25, we did not see a discernible difference among cells transfected with PEI2LA. The lack of an observable effect on the intracellular distribution of PEI2LA complexes in hypertonic media may further suggest that PEI2LA adopts a different mode of intracellular transport than the unmodified PEIs.

4. Discussion

Cellular uptake of complexes can be processed via a number of endocytic pathways; the precise pathways to be utilized is expected to be largely determined by physicochemical properties of the

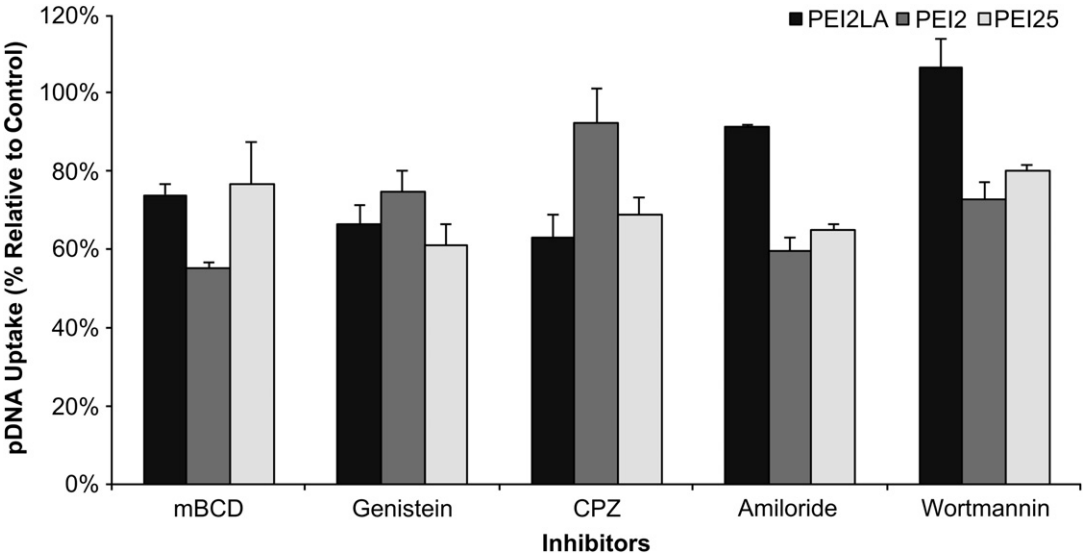

Fig. 7. The effect of endocytic inhibitors on the level Cy3-pDNA uptake of PEI2LA, PEI2 and PEI25 complexes. Cells were pre-treated with the inhibitors for 2 h before transfection and the pDNA uptake was determined 6 h after transfection. The concentrations employed for each inhibitor were noted in the results section. Bar height depicts the relative Cy3-pDNA fluorescent intensity as a percentage of untreated cells.

complexes such as the size, charge, surface features, hydrophobicity or shape [7,29]. Grafting of linoleic acid moieties to the low molecular weight PEI2 renders new physicochemical features to the assembled polymer/DNA complexes, which may alter the uptake pathway in comparison to its unmodified precursor. Indeed, the results presented herein suggest that uptake of the PEI2 complexes depended largely on CvME and macropinocytosis, as pharmacological compounds that either extracted plasma membrane cholesterol, inhibited the activities of tyrosine kinase, phosphoinositide-3-kinase, or membrane Na^+/H^+-ATPase, resulted in significant reduction in both uptake and transfection. In contrast, hydrophobically-modified PEI2LA complexes were taken up

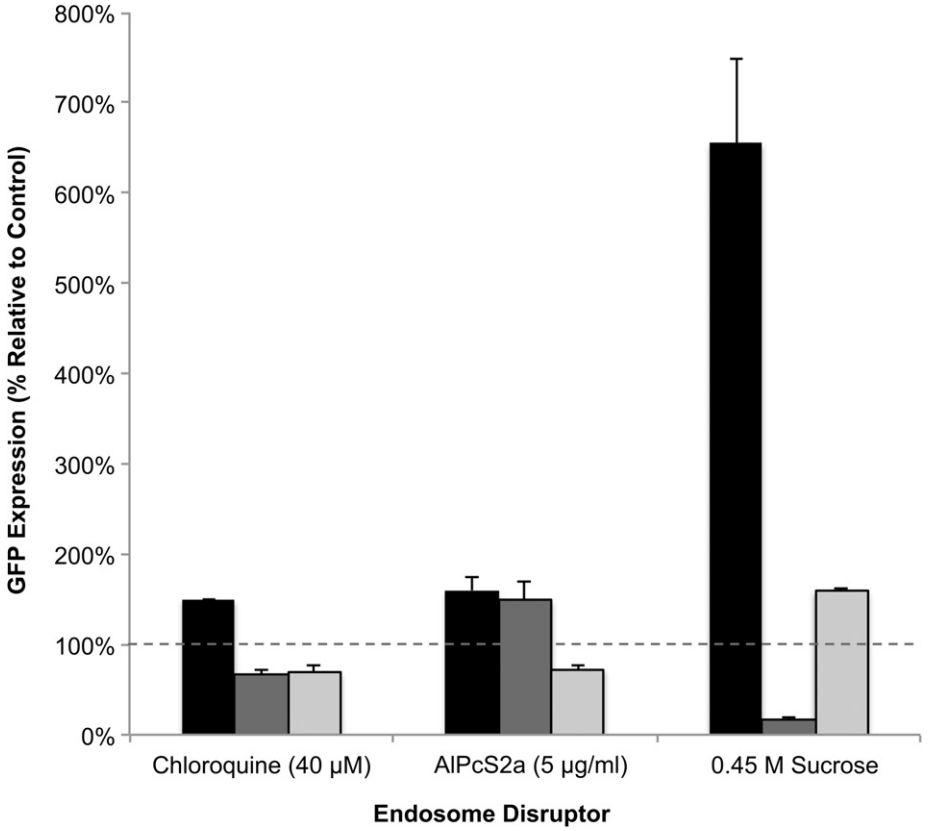

Fig. 8. Effects of the lysosomotrophic agent chloroquine, the photosensitizer AlPcS2a and 0.45 M sucrose on the transfection efficiency of PEI2LA, PEI2, and PEI25 complexes. Bar height depicts the relative fluorescent intensity of transfected cells with the indicated treatment as a percentage of untreated cells. Transection by PEI2LA was increased by 50% following treatment with chloroquine, by 60% following light irradiation of AlPcS2a-loaded cells and by 655% after 0.45 M sucrose treatment.

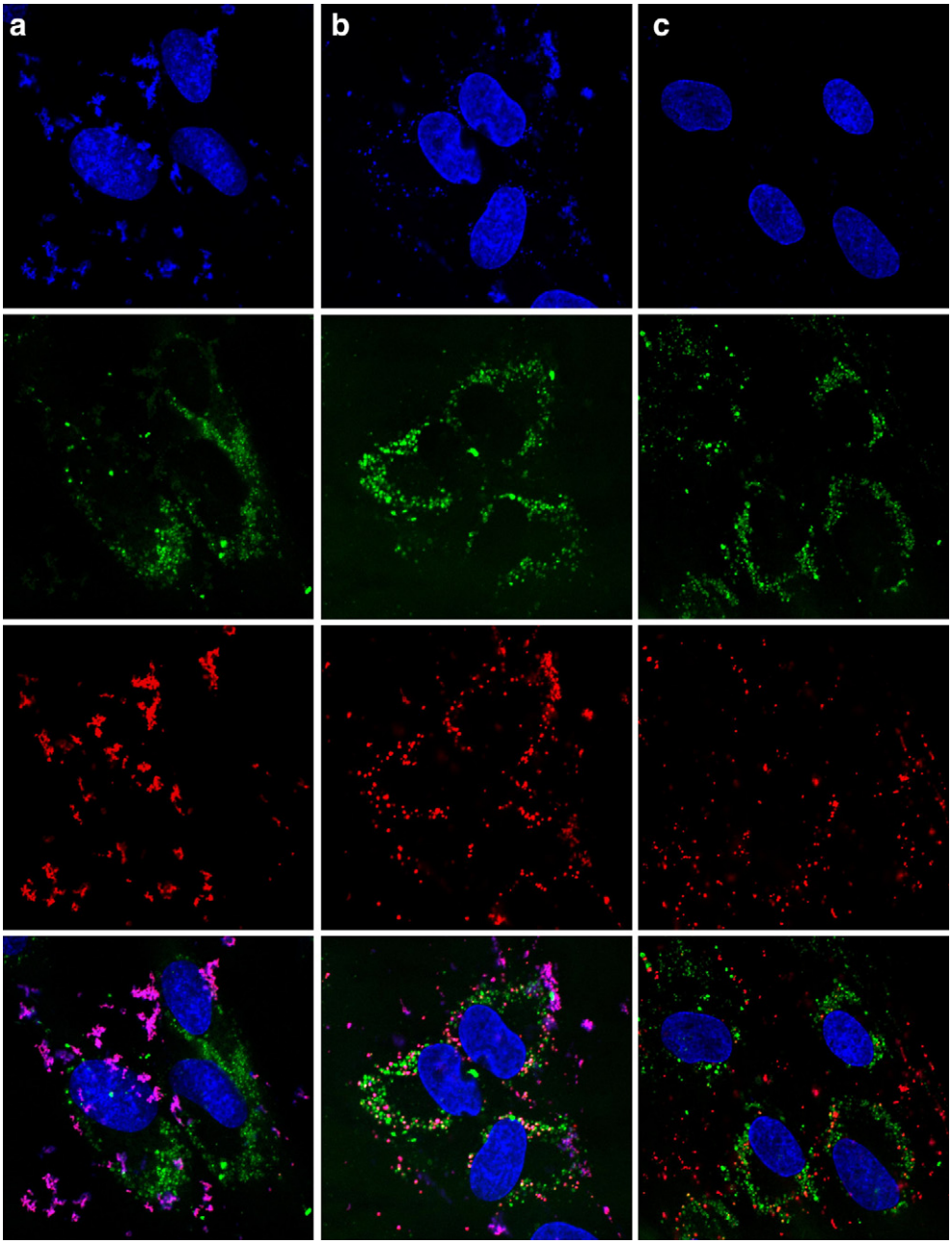

Fig. 9. Fixed-cell confocal microscopy images showing the intracellular distribution of Cy3-pDNA (red) complexes of PEI2LA (a), PEI2 (b) and PEI25 (c). Each image shown on the optical section was representative of the transfected cell population. Cells were stained with Hoechst 33528 and 10 kDa AF488-Dextran conjugate to visualize the nucleus (blue) and the endosomes (green). Purple images are indicative of both Hoechst 33528 and Cy3 stained pDNA. (For interpretation of the references to color in this figure legend, the reader is referred to the web version of this article.)

primarily through the CME pathway, as evident by the faster rate of uptake, a stronger inhibitory effect by CPZ, and enhanced transfection from endosome disruptions, while CvME continued to be involved in the uptake process, albeit to a lesser extent. On the other hand, the uptake profile of PEI25 complexes was different from PEI2 and PEI2LA complexes, and appeared to involve all three endocytic pathways to the same extent since no single pathway stood out as being strongly inhibited. It should be noted that the involvement of the lesser-known clathrin-/caveolin independent pathways in the uptake of these complexes remains to be clarified. In all cases, uptake was not exclusive to a particular pathway, but multiple routes of entry were utilized to varying degrees. Size data obtained by DLS showed bell-shaped distributions in complex sizes, and further suggest that more than one pathways would be required to sufficiently accommodate the uptake of a heterogeneous population of complexes. Microscopy images showed PEI2 complexes to be concentrated around regions excluded from the nucleus, while PEI2LA aggregates were found in and around the nucleus, which stood to be unique from the whole-cell distribution pattern in PEI25. Taken together, the intracellular distribution of complexes complemented the finding from the inhibitor studies, whereby PEI2, PEI2LA and PEI25 each exhibited a distinct profile of uptake pathways.

There are several technical aspects of this study that we consider important to highlight. First, because transfection efficiencies are dependent on the complexation conditions, a single

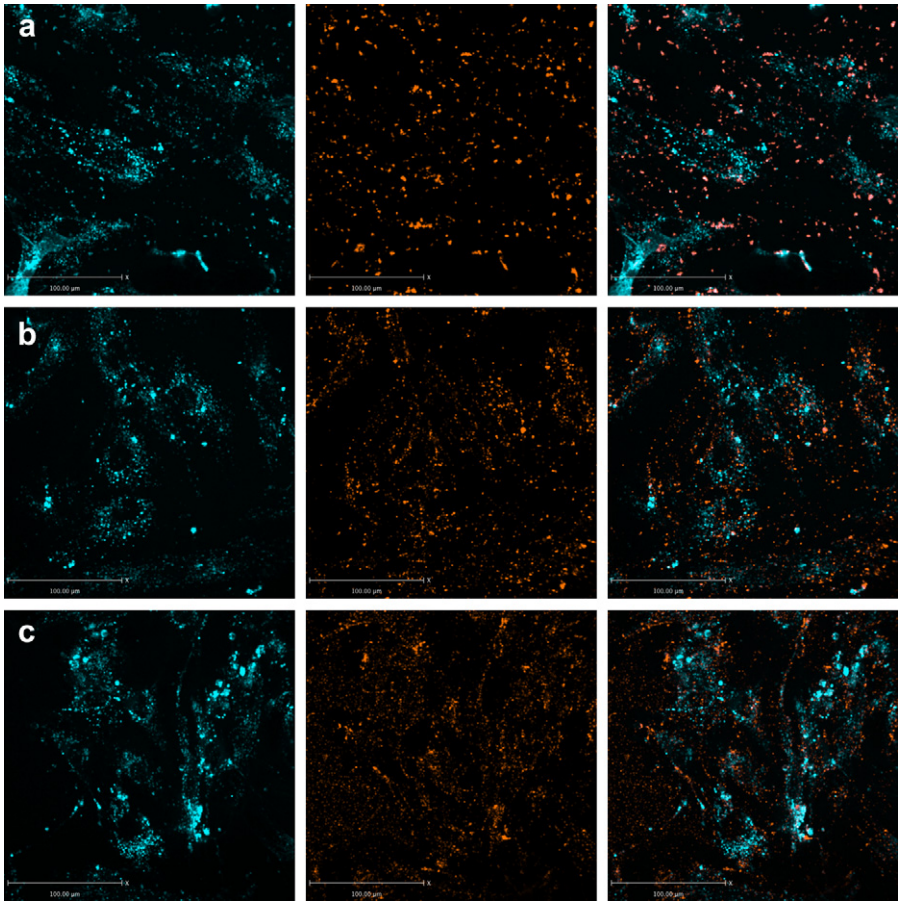

Fig. 10. Live-cell images acquired with a spinning disk confocal microscope of cells transfected with PEI2LA (a), PEI2 (b), and PEI25 (c) complexes. Cell were pre-loaded with the photosensitizer, AlPcS2a (cyan) for 16 h, then transfected with Cy3-pDNA (orange). (For interpretation of the references to color in this figure legend, the reader is referred to the web version of this article.)

complexation method may not accurately portray the relative efficiencies among the GDVs since this will invariably favor one GDV over another [30]. We therefore formulated the complexes in different optimal conditions to ensure the results best reflect the transfection capability of the GDV. Second, there is an inherent delay between the point when complexes are added to the media and the point when complexes reach the cells for internalization. Since complexes formed with different GDVs display different physicochemical properties, this may translate into different sedimentation rates. Aggregation or destabilization of complexes at different rates may further distort the uptake efficiencies [31,32]. We compensated for these variables by applying a centrifugation step immediately following the addition of the complexes to ensure sedimentation rate and complex stability are not limiting the uptake process. Finally, some fluorophores, such as FITC or its derivatives, are sensitive to pH and their fluorescence may be diminished at low pHs [33,34]. Since endosomes and macropinosomes involved in CME and macropinocytosis are known to undergo acidification [7,35], in which the luminal pH of these compartments can drop to 4.3–4.7, we employed a pH-insensitive fluorophore to ensure complexes that are localized in acidic compartments do not result in diminished signal intensity. This is particularly important for studies involving comparative evaluation of novel biomaterials for gene delivery where prior knowledge of the uptake pathways is largely unknown. Overall, we believe these steps should improve the design of future studies on complex uptake and trafficking.

Our results from PS-induced endosome disruption showed improved transfection efficiency for PEI2LA and PEI2. However, the enhancement observed was minimal compared to other studies [36–39]. It should be noted that, in cases of sub-optimal complexation conditions (e.g., low N/P ratio), PSs are expected to be more beneficial in transfection [40,41]. Considering that we optimized transfection conditions for each GDV, it is not surprising that PS did not make a great impact in transfection efficiency. Further, the effectiveness of PS-induced endosome disruption is dependent on the extent of co-localization between the complexes and the PS [42]. The images captured by confocal microscope in this study revealed a lack of spatial coordination between PSs and complexes, confirming that PSs did not promote efficient release of complexes from the endosome. A method to synchronize the intracellular location of PS and complexes may lead to a greater margin of enhancement in transfection.

It is surprising that PEI2LA complexes, despite being the largest, were nevertheless taken up predominantly through CME rather than macropinocytosis, even though CME and CvME are often associated with smaller complexes (up to 200 nm) while macropinocytosis is typically involved with larger complexes (up to 1 μm [13,25,43,44]). Thus, we did not find a correlation between the sizes of our complexes and the reported sizes associated with each endocytic pathways [15,43]. Because uptake pathway is interdependent on physicochemical composition of the complexes and the cell type [14,15,45], direct comparison of results with previous studies based on size alone may not be applicable. Further, size measurements in aqueous environment could be an over-

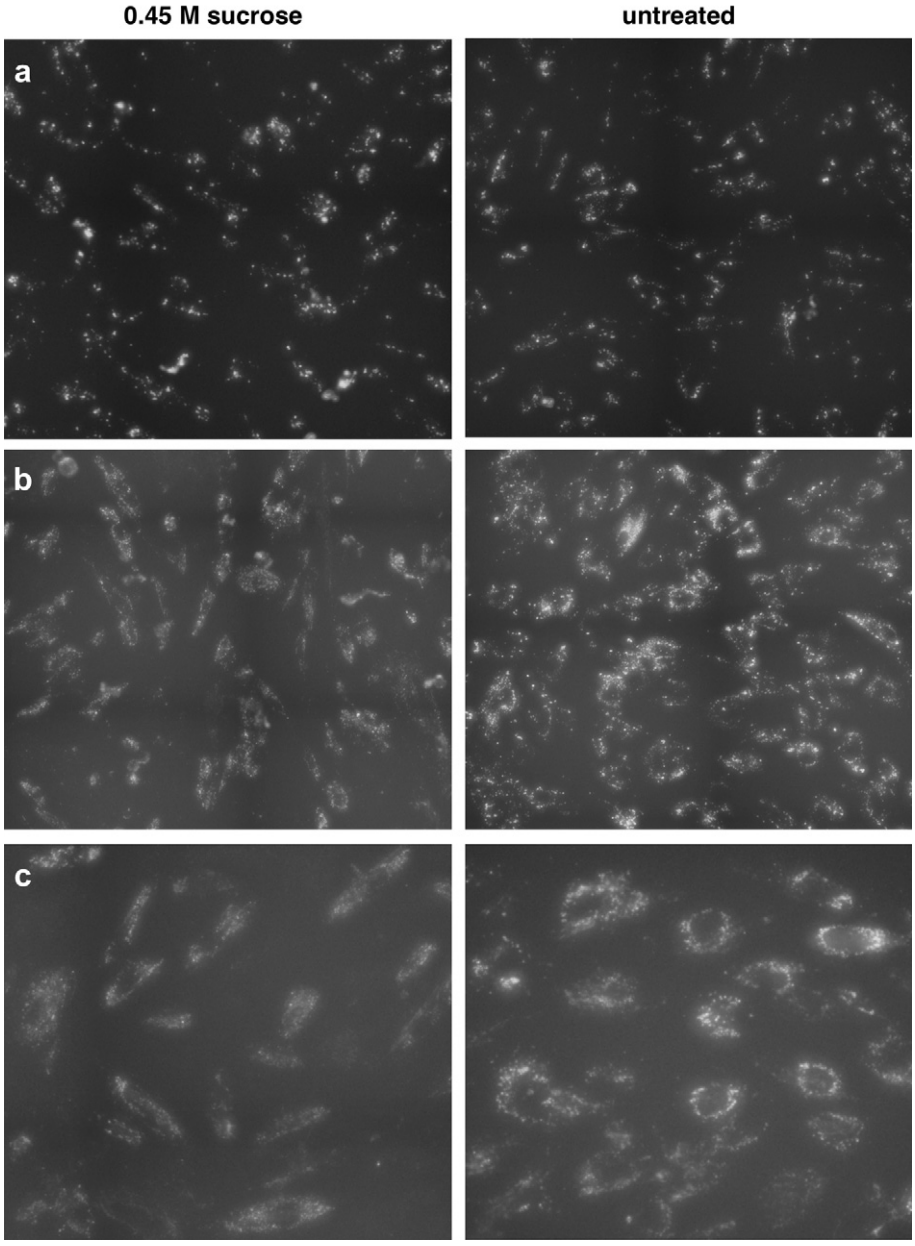

Fig. 11. Wide-field microscopy images of cells pre-treated for 2 h with hypertonic media (0.45 M sucrose in OPTI-MEM, left column) and in OPTI-MEM only (right column), then transfected with PEI2LA (a), PEI2 (b), and PEI25 (c) complexes. Images were captured on live cells grown in a plastic tissue culture plate.

estimation of actual complex size owing to the hydrophobic nature of the complexes, which has a higher tendency towards aggregation, leading measurement to the aggregates of the complexes, rather than individual complex. It is conceivable that size does impose restriction on the uptake pathway, but in a way that allows smaller complexes to utilize a wider range of pathways, whereas larger complexes are restricted to a few specific routes. This notion came from the observation that PEI25 complexes, being the smallest of the three, were sufficiently taken up by all of the pathways examined in this work, whereas the larger PEI2 and PEI2LA, showed a preference for CvME and CME, respectively. Still, the notion that LA moiety could be involved in facilitating receptor-ligand mediated endocytosis cannot be ruled out; further investigation is needed to reveal additional mechanistic role of lipid moieties in uptake.

The fact that CPZ had the greatest impact on the transfection efficiency of PEI2LA may simply imply that a larger proportion of the complexes were taken up through CME. This does not suggest that CME is the most efficient pathway or that this route is responsible for the increase in transfection efficiency of PEI2LA *per se* since the shift to CME may be a mere consequence of the change in the properties of the complexes as a result of LA substitution. The most efficient pathway would need to be determined by actively targeting the complexes to each of the endocytic pathways, in which the pathway with the highest ratio of transgene expression-to-pDNA uptake would be deemed the most efficient. It is conceivable that CME in this case is not the most conducive transfection pathway for PEI2LA and that the enhancement in transfection is principally derived from the small proportion of the complexes released into the cytosolic domain, which were able to mediate highly efficient trafficking for transfection. In other words, the role of lipid-moieties might not be limited to increasing binding affinity to cellular membranes, but to further act as signaling ligand

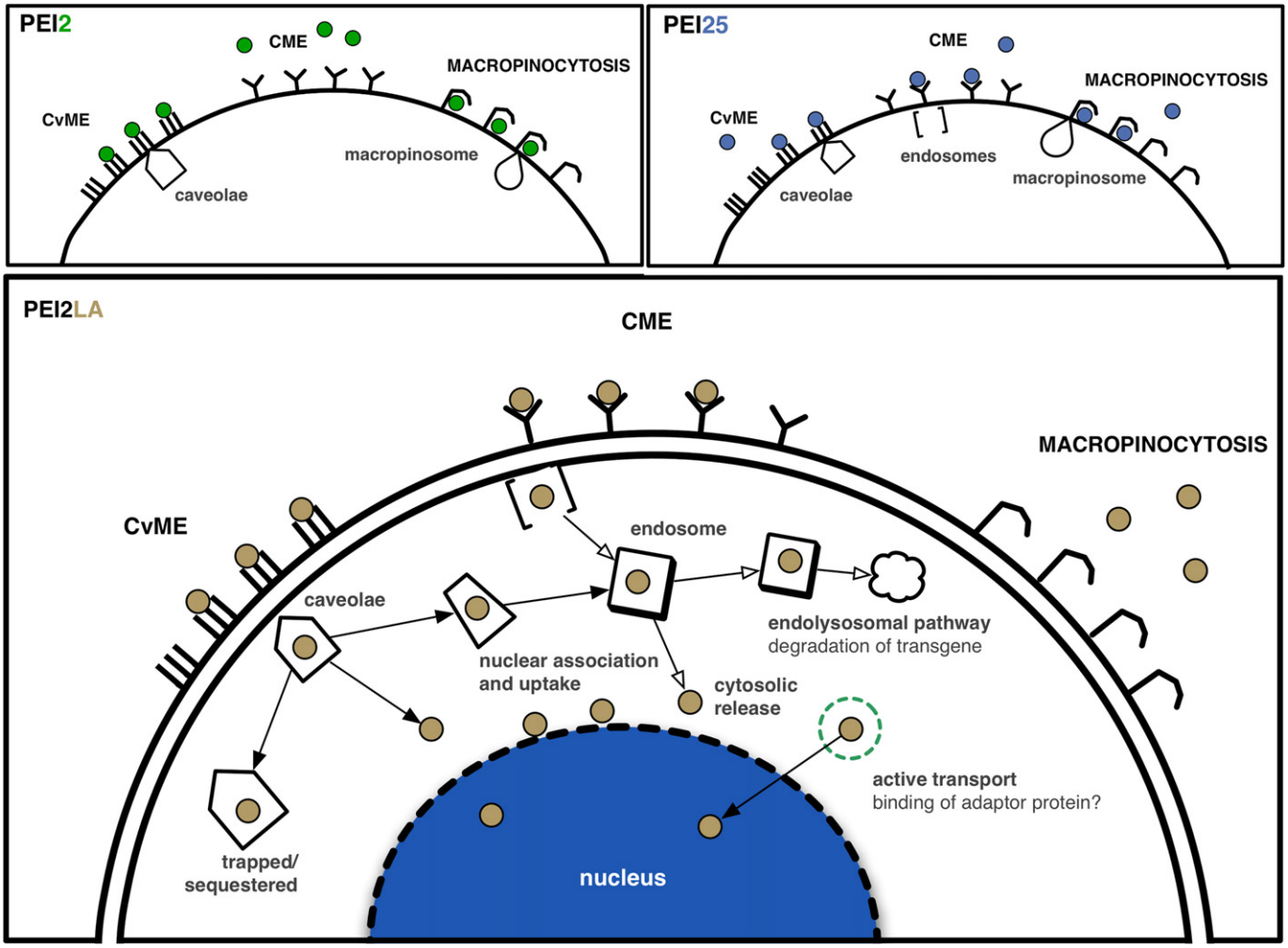

Scheme 1. A proposed model for the uptake and subsequent intracellular trafficking pathway of PEI2LA complexes in NHFF cells. PEI2LA complexes were predominantly taken up through CME, and to some extent by the CvME. Macropinocytosis is either not involved or plays a minor role in the uptake of PEI2LA. PEI2 complexes are internalized mainly through CvME and macropinocytosis while PEI25 are taken up by all endocytic pathways to some extent. Following uptake, endosomes undergoes gradual acidification and are trafficked to the endolysosomal pathway, where the ingested pDNA may become degraded. A portion of the complexes nevertheless is released into the cytosol by yet unknown mechanism(s) and nucleocytoplasmic transport leads to lipid-moieties associating with the lipophilic domains of nuclear membrane. Subsequent nuclear entry is gained by a flip-flop mechanism or passively during cell division when the nuclear membrane breaks down [5].

to mediate active intracellular transport. Endogenous proteins are often post-translationally modified with lipid motifs as transport signal molecule for trafficking to various sub-cellular compartments during organelle biosynthesis or activated metabolic functions [46]. For example, palmitylation allows protein to be targeted to specialized membrane microdomains involved in synaptic scaffolding, signaling and cytoskeletal proteins [47] as well as in retrograde transport during lysosome trafficking [48]. The possibility of lipid moieties acting as a signaling ligand in gene delivery has never been considered. It is likely that an adaptor molecule or lipid binding protein, similar in concept to the transcription factor binding-mediated nuclear transport of nucleic acids via the karyopherin family of proteins, may be employed in the process [49–51]. Additional biochemical and molecular technique is necessary to unravel the mechanistic role of lipids in sub-cellular targeting of GDV conjugates.

Mechanistic studies on the effect of hydrophobic modification are currently limited and the few studies that have been published so far focused primarily on chitosan conjugates. In one instance, the substitution of chitosan with palmitic acid progressively shifted dependence towards lipid-raft mediated endocytosis, as degree of substitution increased [16]. In another instance, glycol chitosan modified with 5β-cholanic acid was found to be taken up by all endocytic pathways and was distributed evenly throughout the cell [52]. Though the cell types and GDVs used in those studies are significantly different from ours, two aspects were consistent with our data; (i) biochemical modification alters the surface properties of the complexes and changes the uptake pathways, and; (ii) complex uptake was not exclusive to one pathway, but employed multiple pathways to varying degrees. The exact uptake pathway by which complexes are taken up is beginning to become less important in recent years as exceptions to their intracellular fate emerge. For example, CvME has often been regarded as the ideal uptake pathway since caveolae are generally non-acidic and non-degradative [53]. However, recent evidence demonstrated that caveolae not only undergo acidification but can also merge with endosome and become destined for the endolysosomal pathway [16,54]. Even macropinocytosis, which is not known to be a degradative path, were recently shown to harbor acidic pH inside macropinosomes and trafficked to the lysosomal pathway [55,56]. The intracellular trafficking in these endocytic pathways may be cell type dependent, making generalization regarding their degradative fate difficult to

arrive. Regardless of the pH or the degradative environment where the complexes end up in, it can be agreed upon that disruption of the vesicular compartment for the eventual cytosolic release is a priority for trafficking to the nucleus. Thus, we believe that subsequent focus in GDV design should be on promoting efficient release into the cytoplasm, rather than targeting to a specific pathway.

Our work presented here provides the first mechanistic view into the transfection pathway of lipid modified PEIs. Scheme 1 shows a proposed model for the uptake and intracellular trafficking of PEI2LA in NHFF cells. Briefly, LA-substituted complexes are taken up predominantly via CME, and to a lesser extent by CvME; macropinocytosis is either not involved or plays a minor role in the uptake. Following release into the cytosol, the LA moieties mediate nuclear import either through association with hydrophobic domain of the nuclear membrane or through fusion to gain direct entry [5]. What remains to be determined is the fate of the complexes within vesicular compartments and the mechanism by which the portion of complexes manage to be released into the cytosol. Existing literature on the uptake pathways of cationic GDVs employed transformed cell lines such as HEK293, CHO, COS-7, and HeLa cells [8–10,18,57]. To the best of our knowledge, this study is the first study to probe transfection pathways of polymeric GDVs in the context of a clinically-relevant primary tissue derived human foreskin fibroblast cells. The results from this study should further facilitate the rational design of non-viral gene delivery systems for clinical applications.

5. Conclusions

Lipid modification to PEI2 alters the cellular uptake pathway of its assembled DNA complexes from one that is predominantly macropinocytosis-driven to pathways that are dependent on CME in primary fibroblast cell culture. The exact pathway responsible for efficient transfection is not clear in this case, but may not be critical to the overall design of GDV, unless methods to promote release into cytosol are coupled to a particular uptake pathway, since endosome escape continues to be a major rate-limiting step even with more-effective lipid-modified polymers. Hydrophobic modifications are thought to enhance transfection by promoting association with lipid components of the plasma membrane and nuclear envelope, but the lipid moieties may have additional roles as transport signals in intracellular trafficking as well. The use of primary tissue-derived cells in this study permits direct translation of research findings to clinical applications, and should be the preferred model, rather than immortal cells, for future evaluation of non-viral GDVs.

Acknowledgments

We are grateful for the financial support from the Natural Sciences and Engineering Research Council (NSERC) and Canadian Institutes of Health Research (CIHR). C. Hsu is supported by the NSERC Alexander Graham Bell Canada Graduate Scholarship. We thank Geraldine Barron (Alberta Health Services), Dr. Xuejun Sun (Department of Experimental Oncology), Dr. Stephen Ogg (Dept. of Medical Microbiology & Immunology) for their assistance with confocal microscopy, and Mr. John Benson (Building and Grounds Services, U. of Alberta) for the fluorescent light fixture.

Appendix A. Supplementary material

Supplementary material associated with this article can be found, in the online version, at http://dx.doi.org/10.1016/j.biomaterials.2012.06.093.

References

[1] Demeneix B, Hassani Z, Behr J-P. Towards multifunctional synthetic vectors. Curr Gene Ther 2004;4:445–55.
[2] Mintzer MA, Simanek EE. Nonviral vectors for gene delivery. Chem Rev 2009;109:259–302.
[3] Incani V, Lavasanifar A, Uludağ H. Lipid and hydrophobic modification of cationic carriers on route to superior gene vectors. Soft Matter 2010;6:2124–38.
[4] Neamnark A, Suwantong O, Bahadur RKC, Hsu CYM, Supaphol P, Uludağ H. Aliphatic lipid substitution on 2 kDa polyethylenimine improves plasmid delivery and transgene expression. Mol Pharm 2009;6:1798–815.
[5] Hsu CYM, Hendzel M, Uludağ H. Improved transfection efficiency of an aliphatic lipid substituted 2 kDa polyethylenimine is attributed to enhanced nuclear association and uptake in rat bone marrow stromal cell. J Gene Med 2011;13:46–59.
[6] Medina-Kauwe LK, Xie J, Hamm-Alvarez S. Intracellular trafficking of nonviral vectors. Gene Ther 2005;12:1734–51.
[7] Khalil IA, Kogure K, Akita H, Harashima H. Uptake pathways and subsequent intracellular trafficking in nonviral gene delivery. Pharmacol Rev 2006;58:32–45.
[8] Rejman J, Bragonzi A, Conese M. Role of clathrin- and caveolae-mediated endocytosis in gene transfer mediated by lipo- and polyplexes. Mol Ther 2005;12:468–74.
[9] van der Aa MAEM, Huth US, Häfele SY, Schubert R, Oosting RS, Mastrobattista E, et al. Cellular uptake of cationic polymer-DNA complexes via caveolae plays a pivotal role in gene transfection in COS-7 cells. Pharm Res 2007;24:1590–8.
[10] Gabrielson NP, Pack DW. Efficient polyethylenimine-mediated gene delivery proceeds via a caveolar pathway in HeLa cells. J Control Release 2009;136:54–61.
[11] Douglas KL. Toward development of artificial viruses for gene therapy: a comparative evaluation of viral and non-viral transfection. Biotechnol Prog 2008;24:871–83.
[12] Hufnagel H, Hakim P, Lima A, Hollfelder F. Fluid phase endocytosis contributes to transfection of DNA by PEI-25. Mol Ther 2009;17:1411–7.
[13] Izumisawa T, Hattori Y, Date M, Toma K, Maitani Y. Cell line-dependent internalization pathways determine DNA transfection efficiency of deca-arginine-PEG-lipid. Int J Pharm 2011;404:264–70.
[14] Douglas KL, Piccirillo CA, Tabrizian M. Cell line-dependent internalization pathways and intracellular trafficking determine transfection efficiency of nanoparticle vectors. Eur J Pharm Biopharm 2008;68:676–87.
[15] Gersdorff von K, Sanders NN, Vandenbroucke R, De Smedt SC, Wagner E, Ogris M. The internalization route resulting in successful gene expression depends on both cell line and polyethylenimine polyplex type. Mol Ther 2006;14:745–53.
[16] Chiu Y-L, Ho Y-C, Chen Y-M, Peng S-F, Ke C-J, Chen K-J, et al. The characteristics, cellular uptake and intracellular trafficking of nanoparticles made of hydrophobically-modified chitosan. J Control Release 2010;146:152–9.
[17] Wang B, He C, Tang C, Yin C. Effects of hydrophobic and hydrophilic modifications on gene delivery of amphiphilic chitosan based nanocarriers. Biomaterials 2011;32:4630–8.
[18] Olton DYE, Close JM, Sfeir CS, Kumta PN. Intracellular trafficking pathways involved in the gene transfer of nano-structured calcium phosphate-DNA particles. Biomaterials 2011;32:7662–70.
[19] Yu J, Vodyanik MA, Smuga-Otto K, Antosiewicz-Bourget J, Frane JL, Tian S, et al. Induced pluripotent stem cell lines derived from human somatic cells. Science 2007;318:1917–20.
[20] Maherali N, Sridharan R, Xie W, Utikal J, Eminli S, Arnold K, et al. Directly reprogrammed fibroblasts show global epigenetic remodeling and widespread tissue contribution. Cell Stem Cell 2007;1:55–70.
[21] Jensen TG. Cutaneous gene therapy. Ann Med 2007;39:108–15.
[22] Wernig M, Meissner A, Foreman R, Brambrink T, Ku M, Hochedlinger K, et al. In vitro reprogramming of fibroblasts into a pluripotent ES-cell-like state. Nature 2007;448:318–24.
[23] Wang J, Dodd C, Shankowsky HA, Scott PG, Tredget EE. Wound healing research group. Deep dermal fibroblasts contribute to hypertrophic scarring. Lab Invest 2008;88:1278–90.
[24] Hsu CYM, Uludağ H. A simple and rapid nonviral approach to efficiently transfect primary tissue-derived cells using polyethylenimine. Nat Protoc 2012;7:935–45.
[25] Conner SD, Schmid SL. Regulated portals of entry into the cell. Nature 2003;422:37–44.
[26] Vercauteren D, Vandenbroucke RE, Jones AT, Rejman J, Demeester J, De Smedt SC, et al. The use of inhibitors to study endocytic pathways of gene carriers: optimization and pitfalls. Mol Ther 2010;18:561–9.
[27] Prasmickaite L, Høgset A, Engesaeter BØ, Bonsted A, Berg K. Light-directed gene delivery by photochemical internalisation. Expert Opin Biol Ther 2004;4:1403–12.
[28] Kato T, Okada S, Yutaka T, Yabuuchi H. The effects of sucrose loading on lysosomal hydrolases. Mol Cell Biochem 1984;60:83–98.
[29] Chavanpatil MD, Khdair A, Panyam J. Nanoparticles for cellular drug delivery: mechanisms and factors influencing delivery. J Nanosci Nanotechnol 2006;6:2651–63.

[30] van Gaal EVB, van Eijk R, Oosting RS, Kok RJ, Hennink WE, Crommelin DJA, et al. How to screen non-viral gene delivery systems in vitro? J Control Release 2011;154:218–32.
[31] Sharma VK, Thomas M, Klibanov AM. Mechanistic studies on aggregation of polyethylenimine-DNA complexes and its prevention. Biotechnol Bioeng 2005;90:614–20.
[32] Ikonen M, Murtomäki L, Kontturi K. Controlled complexation of plasmid DNA with cationic polymers: effect of surfactant on the complexation and stability of the complexes. Colloids Surf B Biointerfaces 2008;66:77–83.
[33] Klonis N, Sawyer WH. Spectral properties of the prototropic forms of fluorescein in aqueous solution. J Fluoresc 1996;6:147–57.
[34] Sjöback R, Nygren J, Kubista M. Absorption and fluorescence properties of fluorescein. Spectrochim Acta Part A Mol Biomol Spectrosc 1995;51:L7–21.
[35] Xiang S, Tong H, Shi Q, Fernandes JC, Jin T, Dai K, et al. Uptake mechanisms of non-viral gene delivery. J Control Release 2011.
[36] Prasmickaite L, Høgset A, Tjelle TE, Olsen VM, Berg K. Role of endosomes in gene transfection mediated by photochemical internalisation (PCI). J Gene Med 2000;2:477–88.
[37] Bøe S, Saebøe-Larssen S, Hovig E. Light-induced gene expression using messenger RNA molecules. Oligonucleotides 2010;20:1–6.
[38] Varkouhi AK, Lammers T, Schiffelers RM, van Steenbergen MJ, Hennink WE, Storm G. Gene silencing activity of siRNA polyplexes based on biodegradable polymers. Eur J Pharm Biopharm 2011;77:450–7.
[39] Nishiyama N, Arnida Jang W-D, Date K, Miyata K, Kataoka K. Photochemical enhancement of transgene expression by polymeric micelles incorporating plasmid DNA and dendrimer-based photosensitizer. J Drug Target 2006;14:413–24.
[40] Bøe S, Longva AS, Hovig E. Evaluation of various polyethylenimine formulations for light-controlled gene silencing using small interfering RNA molecules. Oligonucleotides 2008;18:123–32.
[41] Gargouri M, Sapin A, Arıca-Yegin B, Merlin JL, Becuwe P, Maincent P. Photochemical internalization for pDNA transfection: evaluation of poly(d, l-lactide-co-glycolide) and poly(ethylenimine) nanoparticles. Int J Pharm 2011;403:276–84.
[42] Bonneau S, Morlière P, Brault D. Dynamics of interactions of photosensitizers with lipoproteins and membrane-models: correlation with cellular incorporation and subcellular distribution. Biochem Pharmacol 2004;68:1443–52.
[43] Rejman J, Oberle V, Zuhorn IS, Hoekstra D. Size-dependent internalization of particles via the pathways of clathrin- and caveolae-mediated endocytosis. Biochem J 2004;377:159–69.
[44] Grosse S, Aron Y, Thévenot G, François D, Monsigny M, Fajac I. Potocytosis and cellular exit of complexes as cellular pathways for gene delivery by polycations. J Gene Med 2005;7:1275–86.
[45] Hsu CYM, Uludağ H. Nucleic-acid based gene therapeutics: delivery challenges and modular design of nonviral gene carriers and expression cassettes to overcome intracellular barriers for sustained targeted expression. J Drug Target 2012;20:301–28.
[46] Rajendran L, Kn Ouml Lker H-J, Simons K. Subcellular targeting strategies for drug design and delivery. Nat Rev Drug Discov 2010;9:29.
[47] Fukata Y, Fukata M. Protein palmitoylation in neuronal development and synaptic plasticity. Nat Rev Neurosci 2010;11:161–75.
[48] McCormick PJ, Dumaresq-Doiron K, Pluviose A-S, Pichette V, Tosato G, Lefrancois S. Palmitoylation controls recycling in lysosomal sorting and trafficking. Traffic 2008;9:1984–97.
[49] Miller AM, Dean DA. Tissue-specific and transcription factor-mediated nuclear entry of DNA. Adv Drug Deliv Rev 2009;61:603–13.
[50] Badding MA, Vaughan EE, Dean DA. Transcription factor plasmid binding modulates microtubule interactions and intracellular trafficking during gene transfer. Gene Ther 2011;18:43–52.
[51] Munkonge FM, Amin V, Hyde SC, Green A-M, Pringle IA, Gill DR, et al. Identification and functional characterization of cytoplasmic determinants of plasmid DNA nuclear import. J Biol Chem 2009;284:26978–87.
[52] Nam HY, Kwon SM, Chung H, Lee S-Y, Kwon S-H, Jeon H, et al. Cellular uptake mechanism and intracellular fate of hydrophobically modified glycol chitosan nanoparticles. J Control Release 2009;135:259–67.
[53] Razani B, Woodman SE, Lisanti MP. Caveolae: from cell biology to animal physiology. Pharmacol Rev 2002;54:431–67.
[54] Kiss AL, Botos E. Endocytosis via caveolae: alternative pathway with distinct cellular compartments to avoid lysosomal degradation? J Cell Mol Med 2009;13:1228–37.
[55] Falcone S, Cocucci E, Podini P, Kirchhausen T, Clementi E, Meldolesi J. Macropinocytosis: regulated coordination of endocytic and exocytic membrane traffic events. J Cell Sci 2006;119:4758–69.
[56] Racoosin EL, Swanson JA. Macropinosome maturation and fusion with tubular lysosomes in macrophages. J Cell Biol 1993;121:1011–20.
[57] Mäger I, Langel K, Lehto T, Eiríksdóttir E, Langel U. The role of endocytosis on the uptake kinetics of luciferin-conjugated cell-penetrating peptides. Biochim Biophys Acta 2011;1818:502–11.
[58] Shogomori H, Futerman AH. Cholesterol depletion by methyl-beta-cyclodextrin blocks cholera toxin transport from endosomes to the Golgi apparatus in hippocampal neurons. J Neurochem 2001;78:991–9.
[59] Aoki T, Nomura R, Fujimoto T. Tyrosine phosphorylation of caveolin-1 in the endothelium. Exp Cell Res 1999;253:629–36.
[60] Wang LH, Rothberg KG, Anderson RG. Mis-assembly of clathrin lattices on endosomes reveals a regulatory switch for coated pit formation. J Cell Biol 1993;123:1107–17.
[61] Fretz M, Jin J, Conibere R, Penning NA, Al-Taei S, Storm G, et al. Effects of Na+/H+ exchanger inhibitors on subcellular localisation of endocytic organelles and intracellular dynamics of protein transduction domains HIV-TAT peptide and octaarginine. J Control Release 2006;116:247–54.
[62] Araki N, Johnson MT, Swanson JA. A role for phosphoinositide 3-kinase in the completion of macropinocytosis and phagocytosis by macrophages. J Cell Biol 1996;135:1249–60.
[63] Selbo PK, Weyergang A, Høgset A, Norum O-J, Berstad MB, Vikdal M, et al. Photochemical internalization provides time- and space-controlled endolysosomal escape of therapeutic molecules. J Control Release 2010;148:2–12.
[64] Heuser JE, Anderson RG. Hypertonic media inhibit receptor-mediated endocytosis by blocking clathrin-coated pit formation. J Cell Biol 1989;108:389–400.